cated peptides, two-peptide binding should give rise to combinatorial antigens. That is, although short peptides are probably not immunogenic because of homology with self short peptides (*14*), two short peptides bound to a single class II MHC molecule should be fully immunogenic from the point of view of potential T cell–specific recognition. With respect to the binding of full-length peptides, Bhayani and Paterson have reported the augmentation of an IE^k-restricted cytochrome c peptide–specific response of T cells by a bystander nonstimulatory peptide (*15*). On the basis of these results these authors suggested that two peptides might bind to a single IE^k molecule.

Irrespective of the immunological significance of two-peptide binding to class II MHC $\alpha\beta$ heterodimers, this possible stoichiometry must be recognized in any kinetic analysis of the reactions of MHC molecules with peptides.

REFERENCES AND NOTES

1. R. H. Schwartz, *Annu. Rev. Immun.* **3**, 237 (1985).
2. J. B. Rothbard and M. L. Gefter, *ibid.* **9**, 527 (1991).
3. K. Dornmair *et al.*, *Cold Spring Harbor Symp. Quant. Biol.* **54**, 409 (1990). The transition compact $\alpha\beta \rightarrow$ floppy $\alpha\beta$ for IA^d and IE^k is accelerated at low pH or elevated temperatures or both in both detergent and in lipid bilayers.
4. B. Rothenhäusler, K. Dormair, H. M. McConnell, *Proc. Natl. Acad. Sci. U.S.A.* **83**, 352 (1990). The data in this paper show that FOva(323-339) remains bound to the α and β chains from IA^d for the time period of gel electrophoresis. In recent work the off-rates of FOva(323-339) from separate α and β chains have been measured in detergent solution, and also in lipid bilayers, and have been found to be long, as is the case for the off-rates from the $\alpha\beta$ IA^d heterodimer (R. Tampé, D. Tyvoll, H. M. McConnell, unpublished results).
5. K. Dornmair, B. Clark, H. M. McConnell, unpublished results. Our data on the binding of peptides to IA^d for different truncated peptides are only roughly similar to those of A. Sette *et al.* [*Nature* **328**, 395 (1987)]. This difference is not unexpected since different experiments are involved and none of the results correspond to thermodynamic equilibrium. Also, all of the truncated peptides used in the present work are different since the carboxyl and amino termini are blocked.
6. Abbreviations for the amino acid residues are: A, Ala; C, Cys; D, Asp; E, Glu; F, Phe; G, Gly; H, His; I, Ile; K. Lys; K, Leu; M, Met; N, Asn; P, Pro; Q, Gln; R, Arg; S, Ser; T, Thr; V, Val; W, Trp; and Y. Tyr.
7. Peptide synthesis: The solid-phase technique was used to synthesize Ova(323-339)COOH, Ova(323-328)CONH$_2$, AcOva(323-338)K, AcOva(331-338)K and HSV(8-23) on a Milligen 9050 peptide synthesizer. After purification by high-performance liquid chromatography (HPLC) with a preparative Vydac C$_{18}$ reversed-phase column (Separation Group, Hesperia, CA), peptides were labeled with fluorescein isothiocyanate or Texas Red sulfonyl chloride (Molecular Probes) at the amino terminus or at the ϵ-amino group of the carboxyl-terminal lysine, respectively. The reaction was carried out in dimethylsulfoxide or *N,N*-dimethylformamide in the presence of diisopropylethylamine or 2,6-collidine and monitored by HPLC with an analytical Vydac C$_{18}$ reversed-phase column. After completion, the labeled product was purified with a preparative Vydac C$_{18}$ reversed-phase column. Peptides were characterized by mass spectroscopy.
8. R. Tampé and H. M. McConnell, *Proc. Natl. Acad. Sci. U.S.A.* **88**, 4661 (1991). Similar results have been found by S. N. Witt and H. M. McConnell for the binding of pigeon cytochrome c peptide to IE^k (*ibid.*, in press).
9. T. Förster, *Naturwissenschaften* **6**, 166 (1946).
10. K. Dormair and H. M. McConnell, *Proc. Natl. Acad. Sci. U.S.A.* **87**, 4143 (1990).
11. T. Pedrazzini, A. Sette, M. Albertson, H. Grey, *J. Immunol.* **146**, 3496 (1991).
12. M. F. Perutz, *Nature* **237**, 495 (1972).
13. J. H. Brown *et al.*, *ibid.* **332**, 845 (1988).
14. S. Ohno, *Proc. Natl. Acad. Sci. U.S.A.* **88**, 3065 (1991).
15. H. Bhayani and Y. Paterson, *J. Exp. Med.* **170**, 1609 (1989).
16. Protein isolation: IA^d was isolated and purified as previously described (*4*). The cell line A20.1.11 was used as a source for IA^d. The non-ionic detergent-solubilized membrane proteins were purified by lentil lectin and MKD6-MAb affinity chromatography. After dialysis the final buffer contained 1 mM dodecyl-β-D-maltoside (DM, Calbiochem), 10 mM phosphate buffer, pH 7.0, 150 mM NaCl, and 0.02% NaN$_3$. The preparation was characterized by protein determination and SDS–polyacrylamide gel electrophoresis (12.5% acrylamide).
17. U. K. Laemmli, *Nature* **277**, 680 (1970).
18. J. Heukeshoven and R. Dernick, *Electrophoresis* **6**, 103 (1985).
19. Supported by the Max-Kade Foundation (R.T.) and the National Institutes of Health grant no. 2R37 AI 13587-16. We thank D. Slavazza for synthesis and purification of peptides and D. C. Wiley, R. Huber, and D. Tyvoll for helpful correspondence and discussions.

29 May 1991; accepted 16 July 1991

Periodic Hot-Spot Distribution on Io

ATSUSHI YAMAJI

The Jovian satellite Io has active volcanic hot spots. The point-to-point correlation of the hot-spot distribution indicates that the hot spots preferentially make chains. The arrangement of the chains is periodic with a typical spacing of 120 kilometers. The chains exhibit concordant trends with stresses imposed by the tidal deflection of the lithosphere, suggesting that the hot spots are formed along fissures in the lithosphere. The typical spacing may be controlled by lithosphere thickness.

THERE HAS BEEN A RAPID ADVANCE during the past two decades in our understanding of planetary volcanism (*1*), one of the key phenomena needed to develop models of the internal structure and evolution of terrestrial planets. In this report, I discuss a way to investigate the internal structure by looking into the spatial distribution of volcanoes.

Since the Voyager missions discovered active volcanism on Io, many tens of hot spots have been identified from imaging data (*2, 3*) (Fig. 1). Io is about the size of Earth's moon ($R_{Io} \cong 1820$ km). However, infrared observations show that the satellite discharges as much energy as Earth, and most of the energy emanates from the hot spots (*3, 4*). Jupiter's powerful tides bend and flex the interior of Io as it moves in an eccentric orbit, resulting in frictional heating in the interior and active volcanism (*5*). The tides tend to deform the satellite into a triaxial ellipsoid. The tides with the ellipsoidal symmetry are the engine of Io's tectonics; therefore, the symmetry of surface tectonic features would suggest the dynamic processes going on at depth.

I examined Io's hot-spot distribution using the self-correlation function of discrete points. Self-correlation is defined as

Department of Earth Sciences, College of General Education, Tohoku University, Kawauchi, Sendai 980, Japan.

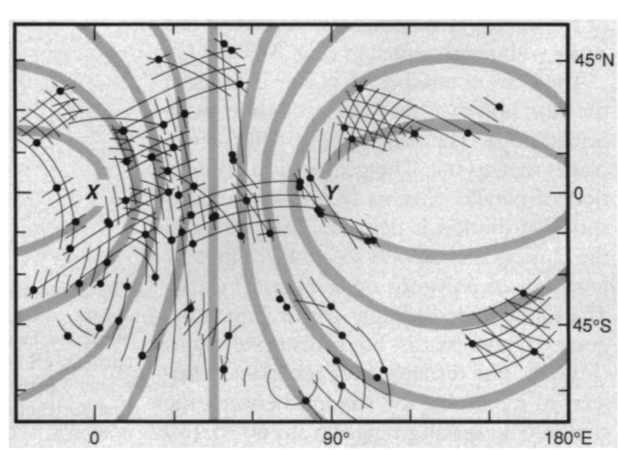

Fig. 1. Mercator projection of hot spots in the eastern hemisphere of Io where Voyager images have the best resolution (*3*). Closed circle, hot spot; thin line, arc on a small or great circle; thick line, stress trajectory induced by the migration of the tidal bulges (*16*). The *X* and *Y* axes point to Jupiter and the trailing direction of the orbital motion, respectively. The *Z* axis points to Iographic north. Three groups of small circles are drawn with the poles 10°N, 133°E; 57°S, 74°E; and 33°S, 7°E. The angular distance between the small circles is constant for each group.

$$C(\mathbf{x}) = \int_{-\infty}^{\infty} h(\mathbf{y})h(\mathbf{y} - \mathbf{x})d\mathbf{y} \qquad (1)$$

for a function $h(\mathbf{x})$ (6). The position of the ith hot spot is denoted by $\mathbf{p}_i$, so that

$$h(\mathbf{x}) = (1/N) \sum^{N} \delta(\mathbf{x} - \mathbf{p}_i) \qquad (2)$$

is an expression of the hot-spot distribution where $\delta(\mathbf{x})$ is the delta function and N is the number of hot spots. For the distribution $h(\mathbf{x})$, we obtain the self-correlation:

$$C(\mathbf{x}) = \frac{1}{N^2} \sum_{i,j}^{N} \delta[\mathbf{x} - (\mathbf{p}_i - \mathbf{p}_j)] \qquad (3)$$

which I call the point-to-point correlation (PPC). Figure 2 shows a graphical expression of the correlation. The PPC corresponds to the disposition of the terminal points of $\mathbf{r}_{ij} \equiv \mathbf{p}_i - \mathbf{p}_j$ for all the couples of i and j with the initial point moored at one position (Fig. 2) (7, 8). Given a certain point $\mathbf{p}_j$, the $\mathbf{r}_{ij}$ values coincide with the positions of the hot spots just translated by $\mathbf{p}_j$, so that a calculation of the PPC involves the translations of the points. If there is periodicity along a certain direction in the hot-spot distribution, the density of the terminal points shows periodic maxima along that direction. Even if the periodic structure has undergone phase modulation, the representative spacing would be marked by the maxima at the sides of the origin $\mathbf{r}_{ij} = \mathbf{0}$. In the case where there is no correlation in the distribution, the terminal points would be randomly plotted and their density would exhibit spherical symmetry.

Figure 3 shows the plot of PPC for the hot spots on Io (9). The plot is by no means random but exhibits an amount of regularity that is surprising in view of the dispersed hot-spot distribution. There are linear clusters across the plot in Fig. 3A as indicated by the arrows, implying that the hot-spot loci have long-distance correlation (~2 R_{Io}). In fact, the linear patterns are side views of planar clusters. The central part of the PPC is taken at close-up range to show the short-distance correlation ($|\mathbf{r}_{ij}| < 0.5\ R_{\mathrm{Io}}$) that brings out the pattern of a lattice with regular spacings (Fig. 3, B and C).

There are a number of planar clusters in the plot; however, they can be classified with orientations. The planes are just like lattice planes in a crystal. The geometrical implication of parallel clusters is simple: the hot-spot distribution is periodic. The points in the clusters correspond to either centers or junctions of polygons on a sphere (Fig. 4). The globe is accordingly paved with polygons; in other words, hot spots make chains (Fig. 1). The distance between planar clusters, Δ, represents the spacing between the chains. The spacing ranges from 60 to 150

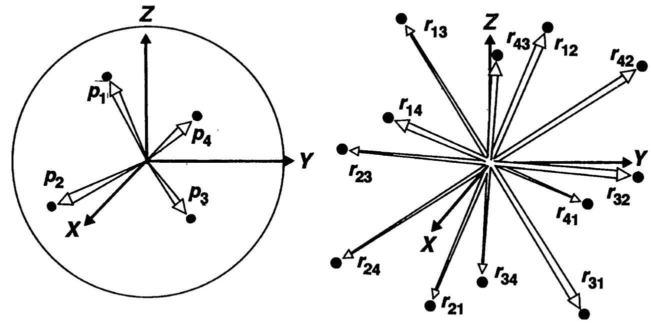

Fig. 2. For the case where there are four points on a sphere (shown by the vectors $\mathbf{p}_1$, $\mathbf{p}_2$, $\mathbf{p}_3$, and $\mathbf{p}_4$ in the left panel), their PPC is made by plotting terminal points of the vectors $\mathbf{r}_{ij} = \mathbf{p}_i - \mathbf{p}_j$ (i, j = 1, 2, 3, or 4) with the same initial point (right panel).

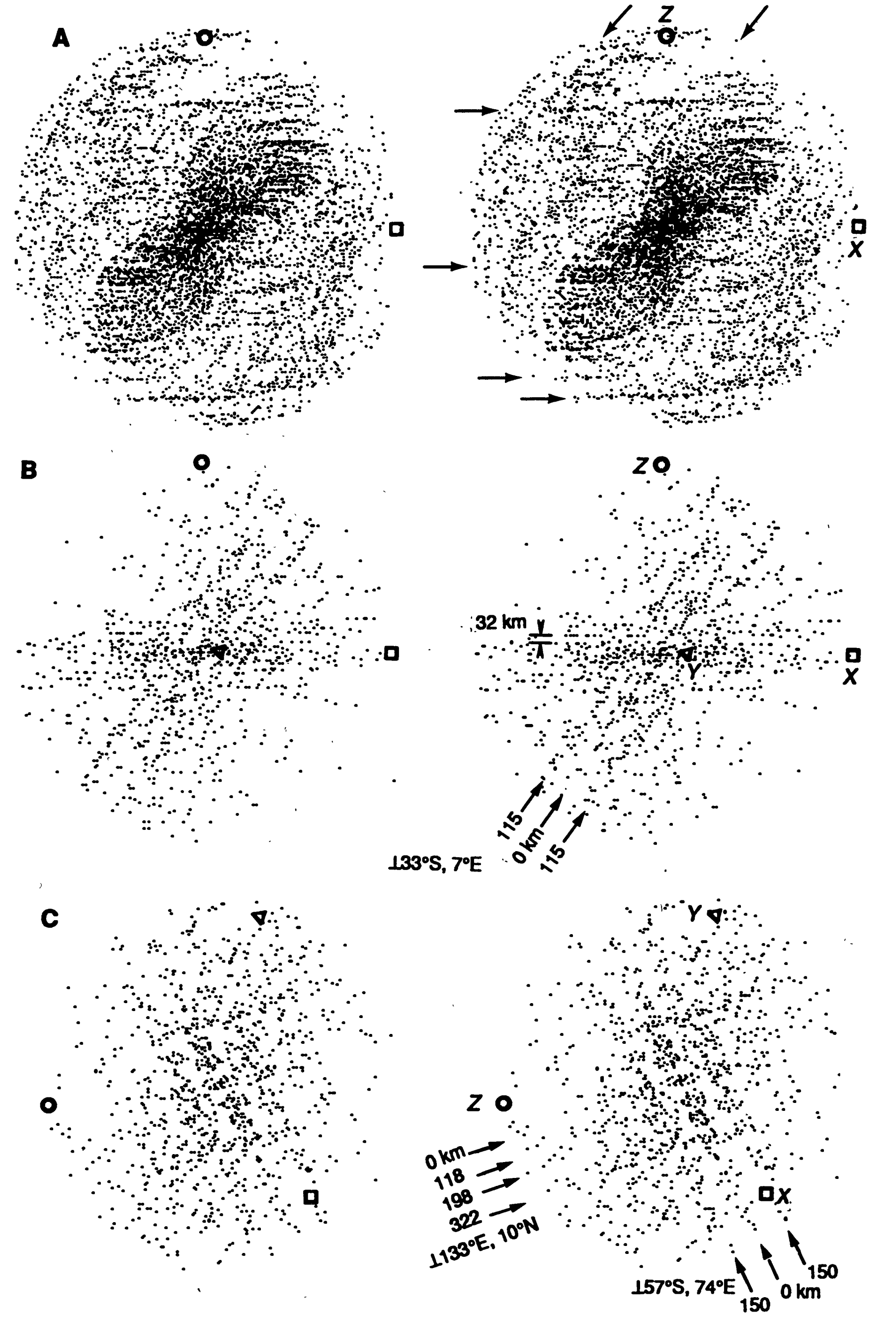

Fig. 3. Stereoscopic pairs showing PPC. Square, triangle, and circle show the direction of the X, Y, and Z axis, respectively. (**A**) Plot of all the vectors $\mathbf{r}_{ij}$ for the hot spots with the marks of X and Z directions at the distance 2 R_{Io} from the center of the plot, viewed from the $-Y$ direction. Arrows indicate planar clusters. (**B** and **C**) Short-distance correlation of the hot-spot distribution ($|\mathbf{r}_{ij}| \leq 0.5\ R_{\mathrm{Io}}$), showing planar clusters with the poles 33°S, 7°E; 10°N, 133°E; and 57°S, 74°E. The periodic hot-spot chains that correspond to those clusters are shown in Fig. 1. The distance of clusters from the origin $\mathbf{r}_{ij} = \mathbf{0}$ is shown.

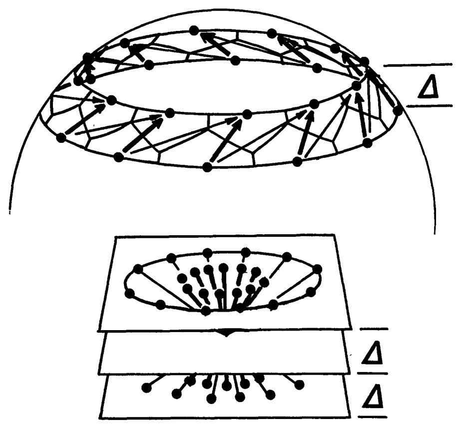

Fig. 4. Schematic showing that points at the centers of a polygonal network on a sphere (upper panel) are mapped into planar clusters in their PPC plot (lower panel). The distance between clusters, Δ, represents the diameter of the polygons.

km, with 120 km the typical spacing.

Self-correlation is independent of phases. This makes the method robust to phase modulation (*6, 7*). Phase modulation in the periodic distribution is shown by the dislocations of the lines of hot spots in Fig. 1.

The precision of the positions of the hot spots delimits the resolution of the present analysis at 32 km (= angular distance 1°). The positions are determined to a precision of 1° (*10*). If we use Cartesian coordinates for latitude and longitude, the spots are plotted at some of the grid points that align at intervals of 1°. The grid pattern is periodic; however, latitude and longitude are actually curvilinear coordinates, and curvature has the same effect as phase modulation in detecting periodicity. The present method is robust to phase modulation. Consequently, the grid pattern is mapped into a lattice in PPC with 32-km spacing.

Looking into the fine structures in the PPC, we see that the short-distance correlation is a more useful approximation than the long-distance correlation because the global distribution of the identified hot spots would be strongly biased by the heterogeneous resolution of the Voyager imaging data. Until the forthcoming Galileo mission, which will make more complete global mapping, the short-distance correlation is appropriate to investigate the organized distribution of hot spots. In the short-distance PPC, points gather about the *XY* plane so that there are a number of hot spots with closely spaced latitudes. However, there is only the pseudoperiodicity with 32-km intervals in this group (Fig. 3B). Although statistical significance is not quantified, there are three groups of parallel clusters with large populations and remarkable periodicity in the PPC (Fig. 3, B and C). The hot-spot chains in Fig. 1 correspond to these clusters.

The volcanic features are geologically young because of the fast sedimentation of volcanic materials at a rate of 0.1 to 1 cm year^{-1} (*11*). The volcanic features are as high as 0.1 to 1 km, so that extinct volcanoes may be buried within 10^4 to 10^6 years. The organized hot-spot distribution is, whatever the mechanism for it, indicative of the recent tectonics of Io.

There could be two explanations for the distribution. First, if hot spots are the surface expression of rising plumes in the mantle as they are on Earth (*12*), organized Bénard convection in the asthenosphere gives rise to a clear correlation (*13*). In this model, the polygons are the manifestation of convection cells, and the diameter of the polygons suggests that the thickness of the convection layer is tens of kilometers, for cell size in Bénard convection is usually a few times the thickness of the convection layer. However, it remains unexplained what determines the alignment of the polygons.

The other explanation is that the hot-spot volcanoes make an array along fissures in the lithosphere, for fracture systems often show parallel and regular spacings. For the fissure model, we could expect azimuths of the hot-spot chains to be controlled by stresses in the lithosphere that are imposed from within and without the satellite. We know little about the intrinsic stress. Extrinsic stress is dominated by Jupiter's tide. The major axis of the tidal ellipsoid lies on the instantaneous Io-Jupiter line. The orbital eccentricity forced by resonant interaction with the other Galilean satellites presumably gives an angular velocity to the spinning of Io that is slightly faster than that of the orbital motion, resulting in the westward migration of the tidal bulges (*14*). The migration induces long-term stresses in the lithosphere (*15*). The thick lines in Fig. 1 show the trajectories of the greatest compressive stresses in the lithosphere (*16*). Extension fractures tend to form nearly parallel to the trajectories (*17*). Many of the chains exhibit concordant orientations with the stress field. Schaber (*18*) reported a number of lineaments and grabens with a variety of azimuths on Io. In addition, he described lava flows from fissures, which are nearly parallel to some of the chains.

Accordingly, the fissure model seems more probable than the convection model. If this is correct, the typical spacing between the chains may be controlled by the lithosphere thickness, because fracture spacing is strongly dependent on the thickness of the brittle layer (*19*).

REFERENCES AND NOTES

1. J. V. Smith *et al.*, *Proc. Apollo 11 Lunar Sci. Conf.* (1970), p. 897; J. A. Wood *et al.*, *ibid.*, p. 965; L. A. Morabito, S. P. Synnott, P. N. Kupferman, S. A. Collins, *Science* **204**, 972 (1979); J. W. Head *et al.*, *ibid.* **252**, 276 (1991).
2. The term "hot spot" as applied to Io is used in a different sense from that for Earth. In plate tectonics, a hot spot causes a sequence of volcanic activity with an age progression. Hot spots on Io are the places of high temperatures that were discovered in the Voyager infrared investigation [R. Hanel *et al.*, *Science* **204**, 972 (1979)]. The spots are identified with volcanoes in imaging data [J. C. Pearl and W. M. Sinton, in *The Satellites of Jupiter*, D. Morrison, Ed. (Univ. of Arizona Press, Tucson, 1982), pp. 724–755].
3. A. S. McEwen, D. L. Matson, T. V. Johnson, L. A. Soderblom, *J. Geophys. Res.* **90**, 12345 (1985).
4. D. Morrison and C. Telesco, *Icarus* **44**, 226 (1980).
5. S. J. Peale *et al.*, *Science* **203**, 892 (1979).
6. R. Bracewell, *Fourier Transform and Its Applications* (McGraw-Hill, New York, ed. 2, 1978).
7. Equation 3 is called the Patterson function in crystallography [J. P. Glusker and K. N. Trueblood, *Crystal Structure Analysis: A Primer* (Oxford Univ. Press, Oxford, ed. 2, 1985)]. The present method is an extension of the Patterson method to a spherical surface.
8. As for Earth's hot spots, the buoyancy flux of each hot spot, a kind of power, is estimated [G. F. Davies, *J. Geophys. Res.* **93**, 10467 (1988); N. H. Sleep, *ibid.* **95**, 6715 (1990)]. Given such a quantity for the *i*th hot spot, w_i, we can weight the point $\mathbf{r}_{ij}$ with the product $w_i w_j$.
9. The 88 hot spots used in this study are taken from the catalog of McEwen *et al.* (*3*) except for the south pole ring. They identified all the spots in imaging data. The ring is removed because positions of volcanic vents are not clear there and the estimate of the surface temperatures of the area is controversial. Namely, McEwen *et al.* argued that the ring is hot. However, recent Earth-based infrared observations show little emission from the region [R. R. Howell, *Bull. Am. Astron. Soc.* **19**, 856 (1987)].
10. Eight hot spots are exceptions. Their coordinates are described down to 0.1° in (*3*).
11. T. V. Johnson and L. A. Soderblom, in *The Satellites of Jupiter*, D. Morrison, Ed. (Univ. of Arizona Press, Tucson, 1982), pp. 634–646; D. B. Nash, M. H. Carr, J. Gradie, D. M. Hunten, C. F. Yoder, in *The Satellites*, J. A. Burns and M. S. Matthews, Eds. (Univ. of Arizona Press, Tucson, 1986), pp. 629–688; M. H. Carr, *J. Geophys. Res.* **91**, 3521 (1986).
12. J. T. Wilson, *Nature* **207**, 343 (1965); W. J. Morgan, *Bull. Am. Assoc. Pet. Geol.* **56**, 203 (1972); N. H. Sleep, *J. Geophys. Res.* **95**, 6715 (1990); M. McNutt, *Nature* **346**, 701 (1990).
13. The theoretical models of Io's internal structure require the existence of a low-viscosity asthenosphere tens or hundreds of kilometers thick [M. N. Ross and G. Schubert, *Icarus* **64**, 391 (1985); M. Segatz *et al.*, *ibid.* **75**, 187 (1988); M. N. Ross *et al.*, *ibid.* **85**, 309 (1990).
14. C. F. Yoder, *Nature* **279**, 767 (1979).
15. R. Greenberg and S. J. Weidenschilling, *Icarus* **58**, 186 (1984).
16. P. Helfenstein and E. M. Parmentier, *ibid.* **53**, 415 (1985).
17. D. T. Griggs and J. Handin, *Geol. Soc. Am. Mem.* **79**, 347 (1960).
18. G. G. Schaber, *Icarus* **43**, 302 (1980); in *The Satellites of Jupiter*, D. Morrison, Ed. (Univ. of Arizona Press, Tucson, 1982), pp. 556–597.
19. B. Vendeville *et al.*, *Spec. Publ. Geol. Soc. London* **28**, 95 (1987); Q. Hang and J. Angelier, *Geol. Mag.* **126**, 355 (1989).
20. I thank D. Jurdy and an anonymous reviewer for helpful comments and suggestions. I benefitted from discussions with M. Toriumi and N. Fujii.

7 February 1991; accepted 1 August 1991